The common reflecting element (CRE) method revisited

J. C. R. Cruz*, Peter Hubral‡, Martin Tygel**, Jörg Schleicher**, and German Höcht‡

ABSTRACT

The common reflecting element (CRE) method is an interesting alternative to the familiar methods of common midpoint (CMP) stack or migration to zero offset (MZO). Like these two methods, the CRE method aims at constructing a stacked zero-offset section from a set of constant-offset sections. However, it requires no more knowledge about the generally laterally inhomogeneous subsurface model than the near-surface values of the velocity field. In addition to being a tool to construct a stacked zero-offset section, the CRE method simultaneously obtains information about the laterally inhomogeneous macrovelocity model. An important feature of the CRE method is that it does not suffer from pulse stretch. Moreover, it gives an alternative solution for conflicting dip problems. In the 1-D case, CRE is closely related to the optical stack. For the price of having to search for two data-derived parameters instead of one, the CRE method provides important advantages over the conventional CMP stack. Its results are similar to those of the MZO process, which is commonly implemented as an NMO correction followed by a dip moveout (DMO) correction applied to the original constant-offset section. The CRE method is based on 2-D kinematic considerations only and is not an amplitude-preserving process.

INTRODUCTION

The ultimate goal of all seismic reflection imaging methods consists of providing a best possible depth image of the subsurface reflectors and possibly deriving their seismic attributes from the signals distributed along the reflector images. It is well accepted that the success with which this task can be achieved highly depends on the accuracy of the velocity model. Different imaging techniques, including the common midpoint (CMP) stack (Yilmaz, 1987), migration to zero offset (MZO) (Dietrich and Cohen, 1993; Tygel et al., 1998), poststack migration (Stolt, 1978; Schneider, 1978), and prestack true-amplitude migration (Bleistein, 1987; Schleicher et al., 1993) require different degrees of accuracy of the macrovelocity model to construct the respective image in either the time or depth domains. Therefore, two key issues to be addressed in seismic reflection imaging are to identify the best imaging technique for an insufficiently known macrovelocity model and to determine how the original estimate of the macrovelocity model can be refined as part of the imaging procedure. To contribute to an answer to this question, we revisit Gelchinsky's (1988) common reflecting element (CRE) method.

Given a set of constant-offset sections, the CRE method is designed to construct a stacked zero-offset section for a 2-D isotropic inhomogeneous earth model starting from a near-surface velocity, assumed constant in the vicinity of each CMP, as the only a priori information. In other words, the CRE method has the same goal as MZO or NMO/dip moveout (DMO). The principal and probably most useful advantage of the CRE method in comparison to CMP and MZO stacks is that it provides, in addition to the stacked section, important parameters for the construction of a macrovelocity model that may even be laterally inhomogeneous. These parameters are given in the form of two specific wavefront attributes that can be assigned to each obtained primary zero-offset reflection event: the radius of curvature R_{NIP} and the emergence angle β_o of a fictitious wavefront Σ_o emerging at the earth's surface (Figure 1, Table 1). The corresponding fictitious wave is assumed to originate at the so-called normal incidence point (NIP) (point C_o in Figure 1), on the target reflector Σ_D. This fictitious wave is referred to as the NIP wave (Hubral, 1983), and its path of propagation $C_o X_o$ is the normal ray. Both the radius

of curvature and the emergence angle of the emerging NIP wave, once assigned to each primary reflection in the stacked section, define what Berkovitch and Gelchinsky (1989; see also Berkovitch et al., 1991; Keydar et al., 1995) call the radiusgram and anglegram sections. In addition to the constructed stacked section, these two auxiliary sections can be used as an input to either generalized Dix-type formulas or more general traveltime or tomographic inversion schemes (Dix, 1955; Hubral and Krey, 1980; Goldin, 1986; Keydar et al., 1995) to generate an accurate macrovelocity model.

The fact that the CRE method needs as an input parameter the near-surface velocity provides no principal difficulty because this is usually available prior to a full velocity analysis. In a marine environment, the water velocity can be used readily. In land seismics, usually some preprocessing such as redatuming (assumed to be done already when the CRE method is to be applied) also needs a near-surface velocity field. If the near-surface velocity is unknown, it can be determined as a result of the CRE method in a more general form of the inversion procedure (Cruz, 1997; Cruz and Martins, 1998).

The CRE method has been studied considerably over the past decade, especially for constructing a stacked section
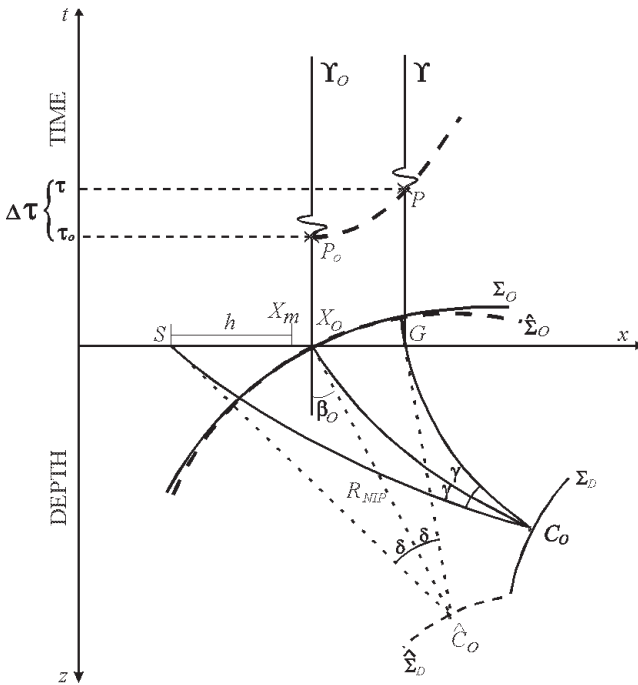
(Rabbel et al., 1991; Steentoft et al., 1992; Steentoft, 1993; Steentoft and Rabbel, 1992a, 1992b, 1994; Gelchinsky et al., 1993a,b; Keydar, 1994; Cruz, 1994) and for estimating a laterally inhomogeneous macrovelocity model (Berkovitch and Gelchinsky, 1989; Berkovitch et al., 1991; Steentoft, 1993; Keydar et al., 1995). The works of Steentoft et al. (1992),

FIG. 1. Sketch of the constant-offset reflection ray SC_oG and the ZO reflection (or two-way normal) ray $X_oC_oX_o$ in a 2-D isotropic inhomogeneous model (solid lines). The (hypothetical) NIP wavefront Σ_o originates at the reflection point C_o and follows the one-way normal ray to the central point X_o, where it emerges under the angle β_o and with a radius of curvature R_{NIP}. All primary reflections from the common reflection point C_o on Σ_D are found at the points $P(x_s, x_g, \tau)$ in the different constant-offset sections. They are aligned along the traveltime curve of the NIP wave, which thus defines the optimal CRE gather and the optimal CRE stacking curve for point C_o. This traveltime curve is estimated from constructing the corresponding situation for the point $\hat{C}_o$ in the auxiliary model with constant velocity and the auxiliary wavefront $\hat{\Sigma}_o$ (dashed lines).

Table 1. List of symbols.

C_o	= Reflection point in the true subsurface model
$\hat{C}_o$	= Center of curvature of the NIP wavefront at X_o
$P(x_m, h)$	= Selected point of the volume of seismic data
$P_o(x_o, \tau_o)$	= Selected point of the simulated zero-offset section
$(R_{\min}, R_{\max})$	= Search interval for the radius of curvature of the NIP wavefront
R_{NIP}	= Radius of curvature of the NIP wavefront at the central point X_o
(S, G)	= Source and geophone points in the seismic line
$U(x_m, h, \tau)$	= Observed seismic trace in the volume of data
$U(x_o, h = 0, \tau_o)$	= Simulated seismic trace in the zero-offset section
$V_{\rm rms}$	= Root-mean-square velocity
$\bar{V}(x_m, \tau_o)$	= Mean medium velocity used in the CMP stack
v_o	= Near-surface constant velocity of the true model, and the velocity of the auxiliary model used in the CRE analysis
X_o	= Selected central point in the seismic line
(x_m, h)	= Midpoint and half-offset coordinate
$(x_o, z = 0)$	= Coordinate of the central point X_o
(x_s, x_g)	= Source and geophone coordinate
Y	= Parameter used in Gelchinsky's formula for determining the CRE gather
$(\alpha_{\min}, \alpha_{\max})$	= Search interval for the asymmetry parameter
α_o	= Asymmetry parameter used to define the CRE gather
β_o	= Emergence angle of the NIP wavefront at the central point X_o
$\Delta\tau$	= True CRE moveout
$\Delta\hat{\tau}$	= Auxiliary (approximated) CRE moveout
$(\Delta\tau_s, \Delta\tau_g)$	= Two true partial CRE moveouts assigned to the source and geophone
$(\Delta\hat{\tau}_s, \Delta\hat{\tau}_g)$	= Two auxiliary (approximated) partial CRE moveouts assigned to the source and geophone
Σ_D	= Reflecting element in the true subsurface model
$\hat{\Sigma}_D$	= Image of the reflecting element in the auxiliary model
Σ_o	= Normal incidence point (NIP) wavefront starting at the reflection point in the true subsurface model
$\hat{\Sigma}_o$	= Circular approximation of the NIP wavefront at the central point X_o
τ	= Traveltime of one primary reflection with arbitrary offset
τ_o	= Traveltime of one normal ray primary zero-offset reflection
$\hat{\tau}$	= Auxiliary (approximated) reflection traveltime

Steentoft and Rabbel (1994), and Olalde (1996) provide a variety of synthetic and field data examples. Steentoft (1993) compares stacked sections generated by CRE and CMP methods applied to the Marmousi data set with impressive results.

Like conventional NMO, the CRE method is based on a second-order approximation of traveltimes. The idea is to make better use of multifold data than CMP sorting can provide. Whereas the second-order traveltime approximation within a CMP gather depends on one parameter only (usually chosen as the NMO velocity), this is not the case in other data subsets. In particular, within the CRE gather to be defined below, the traveltime depends on two parameters, one of which is closely related to the familiar rms velocity. The additional parameter, however, is not of the fourth order (i.e., the next higher order in the traveltime expansion as discussed, e.g., by Al-Chalabi (1973)) but is an additional second-order parameter.

Of course, a more rigorous comparison of stacking methods must include the NMO quartic approximation, but this is not the subject of our work. Here, our interest is to reinforce that the CRE method is certainly more than an exotic pastime for theoreticians. We firmly believe that it should be seen as a worthwhile alternative to a conventional CMP stack. Thus, the main aim of this work is to provide a clear presentation of the CRE method and to point out its importance in the context of other seismic imaging methods.

We stress that the CRE method is designed for inhomogeneous media. For homogeneous media, French et al. (1985) introduce a similar concept they term common reflection point (CRP) stacking, based on the traveltime equation of Levin (1971). They show how to improve CMP stacking to avoid reflection point dispersal. Since CRP stacking is closely related to DMO as well as to the CRE method, the paper of French et al. (1985) is very useful in understanding the relationship between both methods. A generalization of their method is presented by Perroud et al. (1996).

Apart from this introduction and the conclusions, this paper is composed of six principal sections and one appendix. The first section provides the fundamental concepts of the CRE method. In the second section, we present the strategy by which the CRE method constructs a stacked section. The third section describes the three principal implementation steps of the CRE procedure. In the fourth section, the CRE method is tailored to the 1-D case. There, we observe that the optical stack proposed by de Bazelaire (1988), which provides a useful alternative to the standard CMP method, can be viewed as a special case of the CRE method. The fifth section shows why the reflection events in the CRE stacked section do not suffer from pulse stretch. In the sixth section, we provide a high-level view of the main features of the CMP, NMO + DMO, MZO, and CRE stacks to better understand the place of the latter in the framework of zero-offset simulation. Finally, the Appendix provides a brief review of some original CRE formulas that can be compared with the new ones derived in this paper.

BASIC CRE CONCEPTS

We assume the actual subsurface, although unknown, to be well described by a 2-D laterally inhomogeneous isotropic layered earth model. This we call the true subsurface model. We furthermore assume that the kinematics of body waves in this model is well described by zero-order ray theory (Červený, 1987; Červený and Ravindra, 1971; Kravtsov and Orlov, 1990). We next consider a 2-D Cartesian (x, z) system, where the horizontal x-axis is coincident with the seismic line and the vertical z-axis denotes depth (Figure 1). Of the many (not necessarily smooth) reflectors in the true subsurface model, we select one and denote it by Σ_D. We refer to it as the target reflector (Figure 1) and suppose it to consist of small, smooth segments or common reflecting elements.

We further assume that a dense multicoverage experiment has been carried out along the seismic line. This implies that each point of the seismic line is surrounded by a set of shot–receiver pairs (within a certain range of offsets). The discreteness of real-world data may require trace interpolation to substitute missing traces. Each source–geophone pair (S, G) (see Figure 1) is specified by the Cartesian trace coordinates (x_s, x_g) on the x-axis. The corresponding seismic trace is denoted by $U(x_s, x_g, t)$, where $t > 0$ denotes the traveltime. For simplicity, all events in the acquired seismic traces other than P-P primary reflections are considered noise.

Let x_m denote the horizontal Cartesian coordinate of the midpoint X_m between S and G, and let h be the half-offset (Figure 1). Then, the pair (S, G) can be alternatively described by the new coordinate pair (x_m, h). We assume that each pair (S, G) uniquely determines a single P-P primary reflection ray SC_oG, where C_o is the specular reflection point on Σ_D. The corresponding normal ray, i.e., the ray normal to Σ_D at C_o, emerges at the central point X_o with the Cartesian coordinate x_o. Note that, in general, for any given pair (S, G), the points X_m and X_o are not coincident (see Figure 1), i.e., $x_m \neq x_o$.

In multicoverage acquisition geometry, there exists an ensemble of source–receiver pairs that provide P-P reflections from the same point C_o, theoretically including the pair $S_o = G_o = X_o$ (Figure 2). The corresponding ensemble of all seismic traces $U(x_s, x_g, t)$ to these source-receiver pairs is called the true CRE gather of X_o. The true CRE gather generally differs from a CMP gather, coinciding only in cases where $x_m = x_o$ for all pairs (S, G) in the gather. The CRE gather is defined by the CRE trajectory, i.e., the line of tangency between the multicoverage traveltime surface and the stacking surface of Kirchhoff-type prestack depth migration (preSDM), the so-called Cheops Pyramid (Figure 2).

Let us now consider a fixed point C_o and its zero-offset traveltime τ_o along the two-way normal ray $X_oC_oX_o$. For any pair (S, G) belonging to the true CRE gather of X_o, we can write the traveltime τ along the reflection ray SC_oG in the form

$$\tau = \tau_o + \Delta\tau, \tag{1}$$

with $\Delta\tau$ denoting the true CRE moveout.

Referring again to Figure 1, we consider the hypothetical normal-incidence-point (NIP) wave that originates at $t = 0$ from C_o on the target reflector Σ_D (Hubral, 1983). It reaches the seismic line at point X_o at time $t = \tau_o/2$. In fact, this is the exploding reflector concept for one point (NIP) on the reflector. The wavefront at X_o of the emerging NIP wave is subsequently denoted by Σ_o. Let us further denote the emergence angle of the normal ray at X_o by β_o and the radius of curvature of the NIP wavefront Σ_o at X_o by R_{NIP}.

Considering the emerging NIP wavefront Σ_o in the true subsurface model and a source–receiver pair (S, G) pertaining to

the true CRE gather, the true CRE moveout $\Delta\tau$ can be separated as

$$\Delta\tau = \Delta\tau_s + \Delta\tau_g, \tag{2}$$

where $\Delta\tau_s$ and $\Delta\tau_g$ are the two true partial CRE moveouts assigned to points S and G. Both partial moveouts are given by the traveltime difference between the raypaths C_oS and C_oG, respectively, and the one-way normal ray C_oX_o. In Figure 1, $\Delta\tau_s$ is positive while $\Delta\tau_g$ is negative.

Of course, since the subsurface is a priori unknown, so is C_o and thus the true CRE gather and the true CRE moveout. The CRE method offers the possibility of finding a good approximation to the above equation with no other information than the seismic multicoverage data and an estimate of the near-surface velocity v_o at X_o. This velocity is assumed to be constant in the paraxial vicinity of X_o, which includes all sources and receivers of traces in the gather but may vary when another central point is considered. The pair (x_o, τ_o) plays the same role in the CRE method as it does in a CMP stack, i.e., for each central point X_o along the seismic line, the stacking must be done for each time τ_o. The basic difference between the methods is the stacking line. The CMP stacking line, i.e., the moveout hyperbola, lies within the CMP gather and is described by one parameter, the stacking velocity. The CRE stacking line, i.e., the CRE
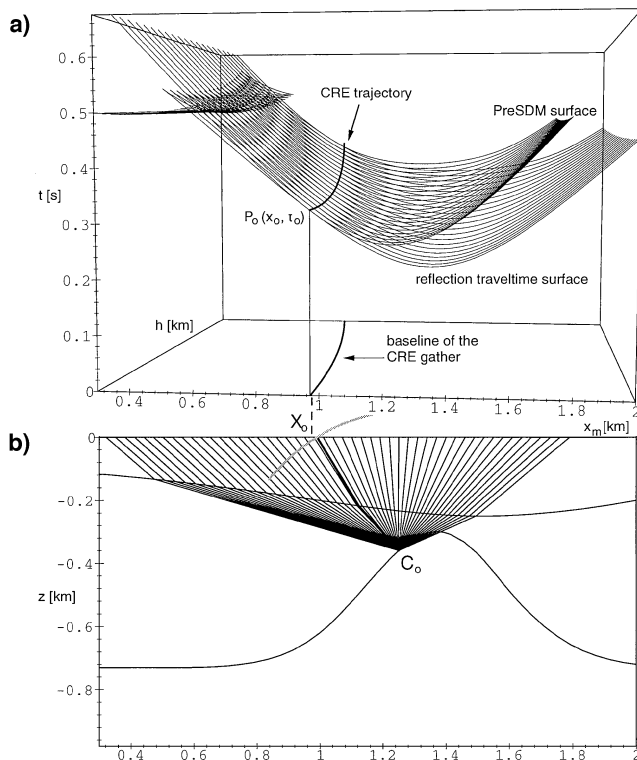

a)

b)

FIG. 2. (a) 3-D multicoverage data space showing the kinematic primary reflection response of the dome in form of CO traveltime curves. Also shown are the CRE trajectory for point (x_o, t_o), the baseline of the corresponding CRE gather, and the preSDM surface (Cheops pyramid) for point C_o. (b) Three-layer model with rays for Kirchhoff-type prestack depth migration (preSDM) of point diffractor C_o. The ZO ray to the reflection point C_o and the circular approximation of the NIP wavefront at X_o are shown in thick black and bold lines, respectively.

trajectory, lies within the CRE gather and is described by two parameters, being the radius of curvature $R_{\rm NIP}$ and emergence angle β_o of the NIP wave.

AUXILIARY CRE GATHER

One of the key ideas of the CRE method is to assign to each central point X_o an auxiliary model, in which the constant velocity coincides with the already estimated velocity v_o at X_o. We stress that this auxiliary model will be used only as a tool to construct the auxiliary CRE gather around X_o and to compute the corresponding auxiliary CRE moveout. No assumptions or restrictions are made on the actual inhomogeneous true subsurface model.

As will be seen, the CRE method will then provide an approximation to the true CRE gather, which we call the auxiliary CRE gather. Within this gather, we have

$$\hat{\tau} = \tau_o + \Delta\hat{\tau}, \tag{3}$$

where $\hat{\tau}$ is the auxiliary CRE traveltime (with $\hat{\tau} \simeq \tau$) and $\Delta\hat{\tau}$ is the auxiliary CRE moveout (with $\Delta\hat{\tau} \simeq \Delta\tau$). Equation (3) is used as a stacking line in the auxiliary CRE gather, in the same way as the NMO traveltime is used for the CMP stack. We will see that for the case of an arbitrarily curved reflector below a constant-velocity overburden, the CRE method provides the exact moveout, i.e., equations (1) and (3) are identical.

Using the auxiliary model, the true NIP wavefront Σ_o can be approximated in the vicinity of X_o by a circular auxiliary NIP wavefront $\hat{\Sigma}_o$. This wavefront has the same radius of curvature $R_{\rm NIP}$ and the same emergence angle β_o as the true NIP wavefront Σ_o at X_o. Its center of curvature $\hat{C}_o$ has thus the polar coordinates given by the NIP wavefront attributes $R_{\rm NIP}$ and β_o (see dashed line $X_o\hat{C}_o$ in Figure 1). In other words, the auxiliary NIP wavefront can be understood as the front of a wave propagating in the auxiliary medium from a point source at $\hat{C}_o$ to X_o.

Let us now see how the auxiliary NIP wavefront can be used to determine the auxiliary CRE gather and the auxiliary CRE moveout. The auxiliary CRE gather is defined by the following fact: for each source-receiver pair (S, G), the two (straight) rays $\hat{C}_oS$ and $\hat{C}_oG$ of the auxiliary NIP wavefront must make up a specular reflection ray $S\hat{C}_oG$ in the auxiliary model. In other words, they are required to make the same angle δ with the normal ray $\hat{C}_oX_o$ (see Figure 1). These two rays then define two auxiliary partial CRE moveouts,

$$\Delta\hat{\tau}_s = \left(\frac{\overline{\hat{C}_oS}}{v_o} - \frac{\overline{\hat{C}_oX_o}}{v_o}\right) \ \text{and} \ \Delta\hat{\tau}_g = \left(\frac{\overline{\hat{C}_oG}}{v_o} - \frac{\overline{\hat{C}_oX_o}}{v_o}\right), \tag{4}$$

the sum of which provides the auxiliary CRE moveout,

$$\Delta\hat{\tau} = \Delta\hat{\tau}_s + \Delta\hat{\tau}_g. \tag{5}$$

Considering that the length of the normal ray is given by $\overline{\hat{C}_oX_o} = R_{\rm NIP}$ and using the law of cosines for the triangles $\hat{C}_oX_oS$ and $\hat{C}_oX_oG$ in Figure 1, we obtain

$$\overline{\hat{C}_oS} = R_{\rm NIP} \sqrt{1 - 2\Delta x_s \sin\beta_o/R_{\rm NIP} + (\Delta x_s)^2/R_{\rm NIP}^2} \tag{6}$$

and

$$\overline{\hat{C}_oG} = R_{\text{NIP}} \sqrt{1 - 2\Delta x_g \sin \beta_o / R_{\text{NIP}} + (\Delta x_g)^2 / R_{\text{NIP}}^2},$$

(7)

where we have introduced the source offset $\Delta x_s = (x_s - x_o)$ and the receiver offset $\Delta x_g = (x_g - x_o)$. Moreover, the emergence angle β_o is assumed to be positive when measured counterclockwise from the vertical axis where $\beta_o = 0$ (Figure 1) and negative when measured clockwise.

Substitution of equations (6) and (7) into equations (4) and taking their sum yields the auxiliary CRE moveout. Returning to equation (3), we obtain the desired expression of the auxiliary CRE traveltime

$$\hat{\tau} = (\tau_o - 2R_{\text{NIP}}/v_o)$$
$$+ \frac{R_{\text{NIP}}}{v_o} \sqrt{1 - 2\Delta x_s \sin \beta_o / R_{\text{NIP}} + (\Delta x_s)^2 / R_{\text{NIP}}^2}$$
$$+ \frac{R_{\text{NIP}}}{v_o} \sqrt{1 - 2\Delta x_g \sin \beta_o / R_{\text{NIP}} + (\Delta x_g)^2 / R_{\text{NIP}}^2},$$

(8)

in terms of the CRE parameters R_{NIP} and β_o as well as the velocity v_o at the central point X_o. Note the explicit dependence on the source and receiver offsets Δx_s and Δx_g, respectively, in the auxiliary CRE gather, as well as on the chosen traveltime τ_o.

Asymmetry parameter

The problem to be addressed now is how to find, in a practical way, all source–receiver pairs of an auxiliary CRE gather with offsets Δx_s and Δx_g for a given set of parameters R_{NIP} and β_o.

By selecting small positive angles δ as in Figure 1 and using simple geometrical considerations, we can express the offsets of the sources and receivers in the auxiliary CRE gather in short-spread approximation as

$$\Delta x_s = -\frac{R_{\text{NIP}} \sin \delta}{\cos(\beta_o + \delta)}, \qquad \Delta x_g = \frac{R_{\text{NIP}} \sin \delta}{\cos(\beta_o - \delta)}.$$

(9)

By eliminating δ from equations (9), one can conclude that the source and receiver offsets must satisfy the equivalent relationships

$$\Delta x_s = \Delta x_g \left[2\Delta x_g \frac{\sin \beta_o}{R_{\text{NIP}}} - 1 \right]^{-1}$$

and

(10)

$$\Delta x_g = \Delta x_s \left[2\Delta x_s \frac{\sin \beta_o}{R_{\text{NIP}}} - 1 \right]^{-1}.$$

We now observe from equations (10) that it is actually the quantity

$$\alpha_o = \frac{\sin \beta_o}{R_{\text{NIP}}}$$

(11)

that controls the relationship between Δx_s and Δx_g. Thus, all points $\hat{C}(R, \beta)$ in the auxiliary model with a fixed parameter value $\alpha = \sin \beta / R$ have an identical auxiliary CRE gather. The specification of one search parameter α instead of two NIP wavefront attributes is therefore sufficient to determine this gather. This fundamental fact was recognized by

Gelchinsky (1988), who termed α the asymmetry parameter (see also Koren and Gelchinsky, 1989; Rabbel et al., 1991). For a prior specified search range of possible wavefront curvatures R, $R_{\min} < R < R_{\max}$, we readily observe (taking into account that $|\sin \beta| \leq 1$) that the asymmetry parameter remains in the interval $-1/R_m < \alpha < 1/R_m$, where $R_m = \min(|R_{\min}|, |R_{\max}|)$.

Using equations (10), the parameter α may be exactly computed from the source and receiver offsets in the auxiliary CRE gather by

$$\alpha = \frac{\Delta x_s + \Delta x_g}{2\Delta x_s \Delta x_g}.$$

(12)

This equation for α differs from the approximate result (A-3) obtained by Gelchinsky (1988) or Rabbel et al. (1991), which is valid for small α only.

The asymmetry parameter α has an interesting geometrical meaning. To understand it, we consider an arbitrary point $\hat{C}(R, \beta)$ in the auxiliary model (Figure 3). At $\hat{C}$, we draw the normal to the line $X_o\hat{C}$ and extend it until its cuts the x-axis (dashed line in Figure 3), thus defining point T at a distance d_t to X_o. By considering the rectangular triangle $X_o\widehat{C}T$ (right angle at $\hat{C}$), we observe that $R = d_t \sin \beta$ and thus $\alpha = 1/d_t$. As a consequence, all search points $\hat{C}$ which, under the same construction, lead to the same point T on the x-axis (i.e., to the same value d_t) give rise to the same auxiliary CRE gather. Conversely, all points $\hat{C}$ pertaining to a fixed CRE gather specified by a given α fall on the lower half-circle through X_o and T with diameter $d_t = 1/\alpha$. Incidentally, this half-circle is nothing else but the so-called Thales circle of seismic depth migration in constant-velocity media presented by Liptow and Hubral (1995) and mathematically described by Schleicher et al. (1997).

It is operationally more attractive (and for the purpose of computing a macrovelocity model also more stable) to use midpoint and half-offset coordinates $h = (x_s - x_g)/2$ and $x_m = (x_s + x_g)/2$ instead of source–receiver coordinates $x_s = x_m + h$ and $x_g = x_m - h$. The asymmetry parameter α as given by equation (12) then takes the form

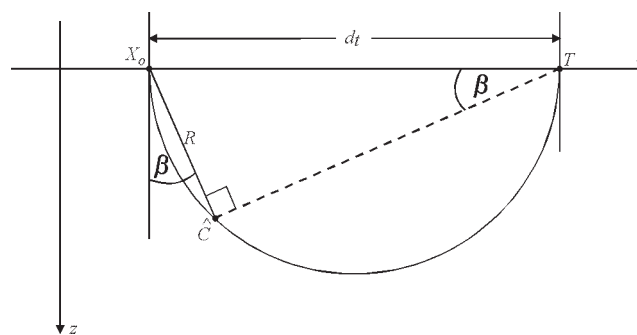$$\alpha = \frac{x_m - x_o}{(x_m - x_o)^2 - h^2}.$$

(13)

FIG. 3. Geometrical meaning of the asymmetry parameter α. Construct for a given search point $\hat{C}(R, \beta)$ in the auxiliary model the normal to the line $X_o\hat{C}$, and extend it (dashed line) until it cuts the x-axis at point T. Using the rectangular triangle $X_o\widehat{C}T$, we see that $\alpha = \sin \beta / R = 1/d_t$. It can be shown that all search points $\hat{C}$ that belong to a given fixed value of α fall onto the lower half-circle through points X_o and T with diameter d_t.

Because we know $|x_m - x_o| < h$, we observe from equation (13) that α always has the opposite sign to $x_m - x_o$. Solving equation (13) for x_m and choosing the physically correct solution, we obtain

$$x_m = x_o + \frac{1}{2\alpha}(1 - \sqrt{1 + 4\alpha^2 h^2}). \qquad (14)$$

This allows us to gather directly from the different constant-offset sections all seismic traces $U(x_m, h, t)$ that belong to the sought-for auxiliary CRE gather for a given value of α.

Up to this point, the CRE method involves no approximation for a curved target reflector Σ_D below a constant-velocity overburden. However, approximating equation (14) for $|\alpha| \ll 1/2h$ or $(x_m - x_o)^2 \ll h^2$, i.e., in short-spread approximation, provides the parabola

$$x_m = x_o - \alpha\, h^2, \qquad (15)$$

which allows us to approximately construct the auxiliary CRE gather for a fixed α. Formula (15) remains a good approximation (with an error less than about 10%) as long as $|x_m - x_o| < h/3$. This may be used as a practical criterion for determining the maximum deviation of the midpoint in relation to the fixed central point coordinate along the seismic line for each constant-offset section.

From equation (14) or its approximation (15), we note that $x_m \neq x_o$ (so that X_m is different from X_o) whenever $\alpha \neq 0$. Moreover, $x_m < x_o$ $(x_m > x_o)$ whenever $\alpha > 0$ $(\alpha < 0)$. This confirms that S and G are localized on opposite sides with respect to X_o in an asymmetric way. Only if $\alpha = 0$, then $x_m = x_o$, i.e., sources and receivers are symmetrically located around X_o.

In Figure 4, the parabola (15) is displayed in the (x_m, h) plane for one fixed x_o and constant α. The respective seismic traces $U(x_m, h, t)$ of the auxiliary CRE gather for this value of α are plotted in vertical direction with their origin $(t = 0)$ on the parabola.

Using midpoint and half-offset coordinates, the auxiliary CRE traveltime $\hat{\tau}$ of expression (8) can be recast into the
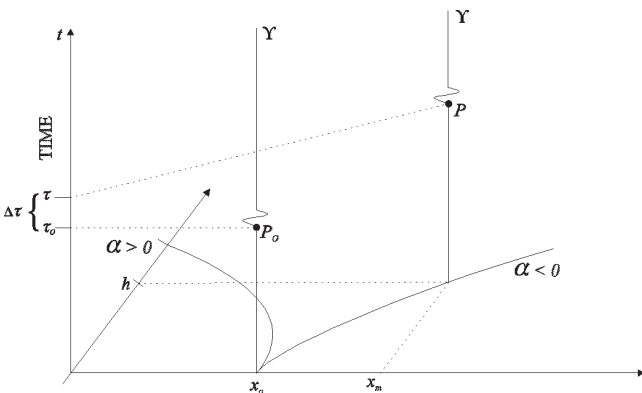

FIG. 4. Construction of a CRE gather in midpoint/half-offset coordinates. For each constant-offset gather, i.e., for each half-offset h, the indicated parabola in the (x_m, h) plane, given by equation (15), defines the midpoint coordinate x_m of that seismic trace $U(x_m, h, t)$ that belongs to the CRE record to be constructed for a given central point X_o. Shown are two parabolas for two different values of the asymmetry parameter α with different signs.

form

$$\hat{\tau} = (\tau_o - 2R_{\text{NIP}}/v_o)$$
$$+ \frac{R_{\text{NIP}}}{v_o}\sqrt{1 - 2\alpha(x_m - x_o + h) + (x_m - x_o + h)^2/R_{\text{NIP}}^2}$$
$$+ \frac{R_{\text{NIP}}}{v_o}\sqrt{1 - 2\alpha(x_m - x_o - h) + (x_m - x_o - h)^2/R_{\text{NIP}}^2},$$
$$(16)$$

where x_m is given by equation (14) or its approximation (15).

We find it convenient to visualize the auxiliary CRE traveltime curve (16) in the following way. Let us assume we are given a dense set of 2-D constant-offset sections characterized by half-offsets h varying over the range $h_{\min} \leq h \leq h_{\max}$. Moreover, let us assume that constant-offset sections have been acquired for all continuously varying midpoints x_m over a fixed interval $x_{\min} \leq x_m \leq x_{\max}$ and for all times t within a certain interval $t_{\min} \leq t \leq t_{\max}$. We now consider a 3-D Cartesian coordinate system (x_m, h, t), in which the available data cover a certain 3-D rectangular volume of points $P(x_m, h, t)$ (Figure 2). Each fixed half-offset h specifies a constant-offset section, which is a planar cut parallel to the $(x_m, h = 0, t)$ plane through this volume. It consists of all traces located at midpoints x_m and determined by source–receiver pairs at (x_s, x_g).

For a chosen point $P_o(x_o, \tau_o)$ we must search for all possible depth points $\hat{C}(R, \alpha)$ in the auxiliary model. For each $\hat{C}$, we must examine those traces whose coordinates (x_m and h) satisfy expression (14) or its approximation (15). We may thus visualize the traveltime curve (16) as a 3-D CRE trajectory of points $P(x_m(h), h, t = \hat{\tau}(x_m(h), h))$ parameterized by h and expression (14) or its approximation (15) as the projection of this 3-D trajectory into the (x_m, h) plane, i.e., the baseline of the CRE gather (Figure 2).

Let us stress once more that in a constant-velocity medium, expression (14) exactly defines the true CRE gather and equation (16) then defines the true CRE traveltime. This feature of the CRE method can be verified analytically by comparing formula (13) and Hale's expression for the reflection-point dispersal in one CMP gather with a dipping reflector (Hale, 1991):

$$(x_m - x_o)^2 - \frac{v_o \tau_o}{2 \sin \beta_o}(x_m - x_o) - h^2 = 0. \qquad (17)$$

Note that for constant velocity, $R_{\text{NIP}} = v_o \tau_o/2$. Thus, recalling definition (11), we find that expressions (13) and (17) are identical. From Hale's work we know that the DMO ellipse satisfies equation (17). This allows us to conclude that, in the same way as DMO, the CRE method compensates correctly for the reflection-point dispersal in a constant-velocity medium.

For a laterally inhomogeneous medium, however, both curves (13) and (16) are no longer exact. In fact, the larger the offset h and the more inhomogeneous the medium, the greater the deviations between the true and auxiliary CRE gathers. As a consequence, the corresponding deviations between the true and auxiliary CRE traveltimes become accordingly larger. A feature of the CRE method is that, for all traces pertaining to the auxiliary CRE gather, the auxiliary CRE traveltime curve approximates the true reflection traveltime τ within that gather quite well. Also note that the reflection points for the source–receiver pairs pertaining to the auxiliary CRE gather

generally lie closely to but not coincide with the true reflection point C_o in the true subsurface model. In other words, similar to constant-velocity DMO, the CRE method suffers from some residual reflection-point dispersal in laterally inhomogeneous media.

CRE STACK

Equation (8) lets us calculate the auxiliary CRE moveout for any given point $\hat{C}_o$ in the auxiliary model for known CRE parameters R_{NIP} and β_o. Correspondingly, equation (16) fulfills the same task given the parameters α and R_{NIP}. The basic idea of the CRE method is now to use the same formulas for a given set of search points $\hat{C}$ in the auxiliary model specified by a certain range of search parameters R and β to find that particular auxiliary NIP wavefront that fits the data best. The process is completely parallel to searching the best fitting parabola or hyperbola, as is done in conventional NMO analysis. However, whereas NMO analysis is carried out on CMP gathers that are already available by simple sorting, the CRE method needs auxiliary CRE gathers that are constructed during the process—with no extra effort. The best fitting CRE traveltime is then specified using a two-parameter (R, β) coherency analysis on the data.

Two-dimensional CRE method algorithm

Given a point $P_o(x_o, \tau_o)$ in the stacked section to be constructed and the velocity v_o at X_o, which will be the velocity of the auxiliary model, the implementation of the CRE method can be subdivided into three steps.

Determination of the auxiliary CRE gather.—First, define the search region $R_{min} < R < R_{max}$ and $\alpha_{min} < \alpha < \alpha_{max}$. Next, introduce a selected α into formula (14) to find in each available constant-offset section, specified by its half-offset h, the midpoint x_m of the source–receiver pair that belongs to the sought-for auxiliary CRE gather. This CRE gather is completely characterized by α. Of course, if the calculated midpoints x_m are not close enough to actual CMP points covered by the acquisition geometry, trace interpolation may be required.

Coherency analysis.—For each pair (R, α), perform a coherency or semblance analysis (see, e.g., Taner and Koehler, 1969; Neidell and Taner, 1971; Gelchinsky et al., 1985) of the auxiliary CRE gather for α along the auxiliary CRE traveltime trajectory (16). Assigning the resulting semblance values to the related search point $\hat{C}$ yields the local semblancegram. This can be scanned for its maximal value (or maximal values), automatically or by an interpreter.

CRE stack.—The maximum semblance value in the local semblancegram determines the optimal values $\alpha = \alpha_o$ and $R = R_{NIP}$ [and thus also $\beta_o = \arcsin(R_{NIP}\alpha_o)$] for point $P_o(x_o, \tau_o)$. These in turn define the optimal CRE gather, as well as the optimal CRE stacking curve (16) along which the trace amplitudes are stacked. The resulting optimal CRE stack is then assigned to $P_o(x_o, \tau_o)$. If there is more than one maxima, the corresponding stack outputs are added to produce the stacked output at P_o. As a result of repeating this process for each point $P_o(x_o, \tau_o)$, the sought-for stacked section is obtained.

Moreover, two NIP-wavefront parameter sections, the radius-gram and the anglegram, defined by the optimal values R_{NIP} and β_o assigned to $P_o(x_o, \tau_o)$, are also obtained as an important byproduct (or maybe even the main product). These two new attribute sections can be used along with the stacked section as input to an inversion procedure based on generalized Dix-type formulas to estimate the macrovelocity model.

We have summarized the CRE method for the case of a single reflection point C_o on a single target reflector Σ_D. Under this assumption, we expected only C_o to provide a significant CRE stack value at $P_o(x_o, \tau_o)$. Similar to the classical CMP method, we need not concentrate on a single target reflector nor on a single reflection point. The above three steps remain unchanged if many reflectors exist and whether or not a particular reflector Σ_D gives rise to more than one ZO reflection at $P_o(x_o, \tau_o)$. If one cannot assign a (sufficiently strong) CRE stack value to $P_o(x_o, \tau_o)$, we assume there will be no primary ZO reflection observed at this point.

Performing a CRE stack by means of the new CRE moveout formula (16) presents some advantages with respect to the original formula introduced by Gelchinsky and co-workers [e.g., Koren and Gelchinsky (1989) or Rabbel et al. (1991); see also equation (A-5)]. The Appendix summarizes Gelchinsky's original formulas and elaborates on the relationship between the two concepts.

Conflicting dips

For the given point $P_o(x_o, \tau_o)$ in the stacked section to be constructed, the two-parameter coherency analysis (e.g., semblance analysis) for pairs (R, β) may possibly find more than one maximum. This problem is pointed out by Rabbel et al. (1991) as a possible source of ambiguities of the coherency criterion used in CRE analysis. There are two possible reasons for multiple semblance maxima: (1) There may be multiple reflection points C_o that contribute to the stack. Each one is associated with a different auxiliary reflection point $\hat{C}_o$. This means that we have more than one auxiliary NIP wave emerging at X_o. This situation is, in fact, analogous to the so-called conflicting-dip problem of the CMP stack. In the CRE stack, this turns out not to be an intractable problem. In fact, each parameter pair (R_{NIP}, β_o) corresponding to each of the obtained semblance maxima can be used independently to construct a corresponding auxiliary CRE gather. The stack is then performed over each of these gathers, and the results are added. In this way, conflicting dips present, in principle, no difficulties to the CRE method. (2) The second possibility is a situation where noisy data result in a couple of maxima for different pairs (R, β), only one of which is correct. In this case, a more sophisticated algorithm (e.g., a genetic algorithm) must be used for a global optimization process to determine the global maximum. The optimal values of R and β are the sought-for parameters R_{NIP} and β_o.

The question of how to perform the two-parameter coherency analysis in a most efficient way has been addressed by several groups. Although further investigations must be carried out, initial results suggest that, at least in two dimensions, the two-parameter search can be realized in a practically feasible way. In this respect, the classical papers of Taner and Koehler (1969), Neidell and Taner (1971), and Gelchinsky et al. (1985) provide worthwhile algorithms. Recent progress

has been reported by Müller et al. (1998) and Berkovitch et al. (1998).

THE CRE METHOD AND THE OPTICAL STACK

The CRE method for a horizontally layered medium

A better insight into the CRE method can be gained upon examining a case of a horizontally layered medium. As an example, we take two horizontal homogeneous layers above one horizontal reflector (see Figure 5). In this case, the CRE and CMP gathers are coincident (i.e., the asymmetry parameter vanishes). Because of the symmetry involved, the NIP wavefront Σ_o reaches G and S at the same time $\tau/2 = \tau_o/2 + \Delta\tau/2$. In other words, the true partial CRE moveouts at S and G are the same, i.e., $\Delta\tau_s = \Delta\tau_g = \Delta\tau/2$. As indicated earlier, the factors $\frac{1}{2}$ in this and the following equations arise because we did not follow the convention of using one-way traveltimes or half-velocities for exploding-reflector considerations. At point X_o, the NIP wavefront Σ_o has the radius of curvature R_{NIP}. Its center of curvature is located at point $\hat{C}_o$, and the emergence angle is $\beta_o = 0$. Setting for simplicity $x_m = x_o = 0$, the resulting CRE traveltime is

$$\hat{\tau} = (\tau_o - 2R_{\text{NIP}}/v_o) + \frac{2R_{\text{NIP}}}{v_o}\sqrt{1 + h^2/R_{\text{NIP}}^2}. \qquad (18)$$

Following de Bazelaire (1988), we introduce the traveltime difference

$$\Delta = \frac{R_{\text{NIP}}}{v_o} - \tau_o/2 \qquad (19)$$

to rewrite equation (18) as

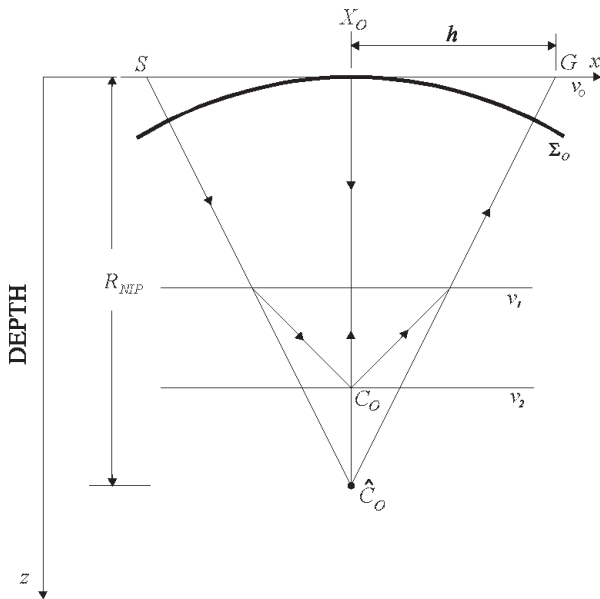$$(\hat{\tau}/2 + \Delta)^2 = (\tau_o/2 + \Delta)^2 + \frac{h^2}{v_o^2}. \qquad (20)$$

Formula (20) represents a hyperbola with its center at $(\hat{\tau} = -\Delta, h = 0)$. For a homogeneous medium with velocity v_o and a horizontal reflector, we have $\Delta = 0$, so that expression (20) corresponds to the familiar hyperbolic NMO traveltime curve with its center at $(\hat{\tau} = 0, h = 0)$.

As noted by Cruz et al. (1995, 1996), formula (20) is a well-known result previously derived by de Bazelaire (1988), who obtained it for layered media with curved (circular) interfaces from geometrical-optics concepts. As shown in the cited papers, formula (20) is an alternative to the small-offset hyperbolic traveltime approximation (the so-called NMO curve) considered in the standard NMO method,

$$(\tau_n/2)^2 = (\tau_o/2)^2 + \frac{h^2}{V_{\text{rms}}^2}, \qquad (21)$$

where τ_n is the NMO traveltime and $V_{\text{rms}} = \sqrt{2R_{\text{NIP}}v_o/\tau_o}$ denotes the rms velocity related to R_{NIP} and τ_o (Hubral and Krey, 1980). The stack result obtained by means of formula (20) is called the optical stack (de Bazelaire, 1988).

For the considered two-layer model, we have constructed the CRE stacking line to compare it to the corresponding NMO curve (which is known to be a good approximation to the true reflection time in this case). The two hyperbolas given by expressions (20) and (21), i.e., the CRE and NMO curves, respectively, are displayed in Figure 6 together with the true reflection traveltime (labeled Fermat curve). In our example, we considered a homogeneous half-space overlain by two horizontal layers, the first with a thickness of $H_o = 1000$ m and the second with $H_1 = 500$ m. The velocities in the layers are $v_o = 2000$ m/s and $v_1 = 2500$ m/s, respectively (see Figure 5). For this model, we also have $V_{\text{rms}} = 2154.73$ m/s, $R_{\text{NIP}} = 1625$ m, and $\Delta = 112.5$ ms. The NMO curve, hyperbola (20), is centered at the origin of the (t, h) coordinate system, while the CRE curve, hyperbola (21), has its center dislocated on the time axis at $t = -225$ ms. In

FIG. 5. Horizontal two-layer model and horizontal reflector. The hypothetical NIP wavefront Σ_o originates at the common reflection point C_o, which corresponds to the auxiliary common reflection point $\hat{C}_o$.
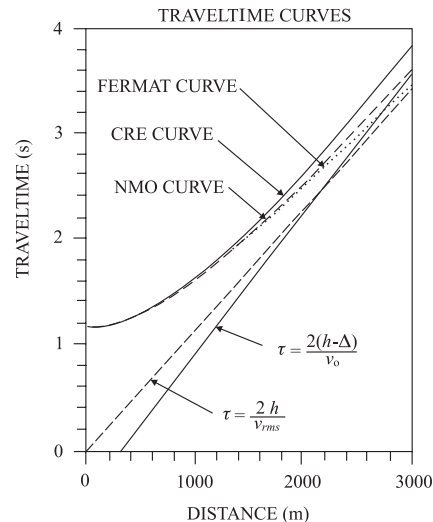

FIG. 6. Traveltime curves calculated for cases of NMO and CRE moveout, considering a model of two layers over a half-space (Figure 5). For the NMO moveout, we used the rms velocity of $V_{\text{rms}} = 2154.73$ m/s, while for the CRE moveout we considered the radius of curvature $R_{\text{NIP}} = 1625$ m, the near-surface velocity $v_o = 2000$ m/s, and $\Delta = 112.5$ ms.

the usual seismic range of half-offsets h (i.e., between 0 and 1500 m), both curves are almost coincident. They also fall together with the Fermat curve, i.e., approximations (20) and (21) are equivalent. This confirms that the CRE stack is a true alternative to the CMP stack, even in the case where the CMP should perform at its best, i.e., when no reflection-point dispersal is present.

At this point, it may be interesting to comment on the accuracy of these approximations for larger offsets. Figure 6 shows that, in this example, the NMO curve is a more accurate approximation than the CRE curve. This is because in a horizontally layered medium, the deviation of the emerging wavefront (which gets increasingly flatter) from a circular one becomes significant. However, de Bazelaire (1988) shows that, for laterally inhomogeneous media (e.g., a horizontal reflector below a circular interface), formula (20) may yield comparable or even better approximations to the true reflection traveltime than the conventional NMO hyperbola (21).

Delayed CRE formula

Starting from the CRE stack formula (16), we can derive a new approximation for the squared CRE traveltime that is very similar to equation (20). This approximation is useful for the case of small offsets and arbitrary overburdens. To get this new squared CRE traveltime approximation, we only need to delay half the original traveltime of the CRE stack, equation (16), by de Bazelaire's (1988) quantity Δ defined in equation (19) and thereafter square both sides of the resulting equation. For small offsets $2h$, we arrive after some straightforward manipulations at the following expression for the squared CRE traveltime:

$$(\hat{\tau}/2 + \Delta)^2 = (\tau_o/2 + \Delta)^2 + \frac{h^2}{v_o^2} - \frac{R_{\text{NIP}}^2}{2v_o^2}(1 - \sqrt{1 + 4\alpha^2 h^2}). \tag{22}$$

By comparing this equation to formula (20), we see that the only difference is the additional third term on the right-hand side of equation (22). Moreover, for an asymmetry factor α equal to zero, i.e., for a vertically emerging NIP wave, equation (22) reduces to formula (20).

Relationships of the CRE and CMP formulas

Our results show that the CRE formula and the so-called delayed hyperbola [equation (20)] are identical for a vertical incident normal ray, i.e., for $\beta_0 = 0$. To get the NMO hyperbola [equation (21)] one only has to perform a second-order Taylor expansion of $\hat{\tau}^2$ in equation (20) with respect to h. Moving to the more general case of arbitrarily curved reflectors in an inhomogeneous medium, Höcht et al. (1999) show that the CRE formula offers a basis upon which to derive the delayed hyperbola and the NMO hyperbola in the CMP gather. This is done by means of CRE trajectories and a hyperbola in the ZO section, whereby one can construct a moveout surface in the multicoverage data set that also accounts for the reflector's local curvature. Performing different Taylor expansions of this surface and restricting them to their second-order representations in the CMP gather yields the hyperbolas in the CMP gather.

PULSE STRETCH

In this section, we compare the stretching effects of the CRE method to those of conventional NMO. For the geometrical considerations, we refer to Figure 7. When constructing a stacked section, the amplitude value of a finite-offset reflection pulse recorded at time $t = \tau$ is assigned to the ZO traveltime $t = \tau_o$. Correspondingly, the value recorded at $\tau + \delta\tau$ is assigned to $\tau_o + \delta\tau_o$. Since the small intervals $\delta\tau$ and $\delta\tau_o$ are not identical, the seismic pulse is stretched by this process. Quantitatively, this stretch can be described by a factor $\mathcal{F}$ given by the ratio between the new length $\delta\tau_o$ and the old length $\delta\tau$ of the pulse. For small intervals $\delta\tau$ and $\delta\tau_o$, this ratio may be replaced by the derivative, namely

$$\mathcal{F} = \frac{d\tau_o}{d\tau} = \left(\frac{d\tau}{d\tau_o}\right)^{-1}. \tag{23}$$

Equation (23) for the pulse stretch factor $\mathcal{F}$ can be obtained directly in a less heuristical manner by the ratio between the instantaneous frequencies of the analytical signal calculated before and after applying the moveout correction (Barnes, 1992). Let us now compare the pulse stretches resulting from NMO correction and CRE moveout. To obtain a quantitative result, we restrict our analysis of the NMO stretch to the 1-D situation described in the previous section. The CRE stretch is analyzed for the general 2-D situation.

NMO stretch.—In the 1-D case, the pulse stretch factor $\mathcal{F}_{\text{NMO}}$ is obtained by computing the derivative of the NMO correction formula (21) and taking the inverse of the result. The result is (see also Vermeer, 1990)

$$\mathcal{F}_{\text{NMO}} = \frac{\tau V_{\text{rms}}^3}{\left(V_{\text{rms}}^3 \tau_o - 4h^2 V_{\text{rms}}'\right)}, \tag{24}$$

where $V_{\text{rms}}' = dV_{\text{rms}}/d\tau_o$. Assuming that $V_{\text{rms}}' \simeq 0$, i.e., that V_{rms} is nearly constant for small changes of τ_o, equation (24) reduces to the well-known expression (Yilmaz, 1987)

$$\mathcal{F}_{\text{NMO}} = \frac{\tau}{\tau_o} = \sqrt{1 + \frac{4h^2}{V_{\text{rms}}^2 \tau_o^2}}. \tag{25}$$
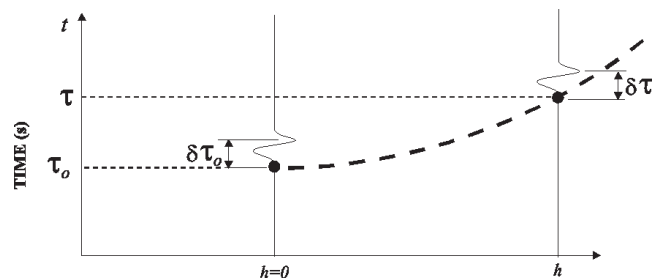

FIG. 7. To construct a primary ZO reflection in the desired stacked section, the primary constant-offset reflection recorded at a time $t = \tau$ must be moved to the traveltime $t = \tau_o$. If by this process a small time interval $\delta\tau$ in the original constant-offset section is mapped onto a small time interval $\delta\tau_o$ in the constructed stacked section, the corresponding seismic pulse suffers a stretch of $\delta\tau_o/\delta\tau$.

In fact, after applying the NMO correction to the reflection data, the frequency content of the primary reflection pulse is decreased by the factor $\mathcal{F}_{\text{NMO}}$, i.e., its length is increased by this factor.

CRE stretch.— In contrast, the CRE stretch factor $\mathcal{F}_{\text{CRE}}$ resulting from performing a CRE moveout is obtained by applying the derivative with respect to τ_o to the CRE traveltime [equation (16)]. At this point, it is crucial to note the fundamental difference between the NMO time [equation (21)] and the CRE time [equation (16)]. Whereas the NMO time is a given τ_o-dependent approximation to the correct stacking line, the optimal CRE stacking line is determined independently for each value of τ_o by coherency analysis. Thus, the optimal radius of curvature R_{NIP} of the NIP wavefront and its optimal angle of emergence β_o will remain the same for each primary finite-offset reflection. These parameters are thus independent of τ_o as long as τ_o belongs to the same reflection in the stacked section to be constructed. This means that as long as we consider the same reflection event, the CRE moveout curves will remain parallel. As a consequence, the CRE correction will not stretch the wavelet. Hence, in mathematical terms, the CRE moveout $\Delta\hat{\tau}$ is independent of $\hat{\tau}_o$, and the stretch factor is therefore given by

$$\mathcal{F}_{\text{CRE}} = \left(\frac{d(\tau_o + \Delta\hat{\tau})}{d\tau_o}\right)^{-1} = \left(\frac{d\tau_o}{d\tau_o}\right)^{-1} = 1. \quad (26)$$

This also means that the frequency content before and after applying the CRE moveout is preserved and no stretch effect is observed. In practice, of course, because of noisy data, the coherency analysis will not always lead to identical parameters R_{NIP} and β_o for all values of τ_o within one reflection in the constructed stacked section. In most situations, however, the obtained parameters will be sufficiently close together to keep all stretch effects negligible. However, regions with low coherency will suffer from additional stretch.

COMPARISON WITH OTHER METHODS

Table 1 displays the main features of four different methods to construct a stacked section, namely, the CMP, NMO/DMO, CRE, and MZO stacks. Underlying is the assumption that all methods are applied to a 2-D laterally inhomogeneous medium. Concerning the CMP stack, let us recall that the re-

sulting stacking velocities $V_s(x_m, \tau_o)$ can only be used to independently construct a (1-D) velocity–depth function for each CMP X_m, thus distorting the lateral inhomogeneities of the velocity model. On the other hand, the wavefront attributes R_{NIP} and β_o obtained by the CRE method allow us to construct a consistent laterally inhomogeneous macrovelocity model. The price to be paid for this increase in accuracy is, of course, a more expensive procedure when searching for two parameters instead of one.

Let us now briefly comment on direct MZO and NMO/DMO. A 2-D, direct MZO (e.g., Tygel et al., 1998) needs a macrovelocity model $v(x, z)$ that should be as accurate as possible. By ray tracing, the MZO operators are determined for each constant-offset section; thus, the best possible simulated ZO section is obtained from each constant-offset section. These must be stacked to simulate a stacked section that can be compared with that obtained by a CMP or CRE stack. This fact is accounted for by the Standard Output row in Table 2. The 2-D direct MZO is probably the most expensive method. The cheaper, approximate process consisting of NMO/DMO is, on the other hand, absolutely equivalent to a direct MZO in a constant-velocity medium only. However, also in slightly inhomogeneous media, NMO/DMO has been proven to be a successful operation. This process needs some given estimate of a mean medium velocity $\bar{V}(x_m, \tau_o)$ (assumed to be constant for a given CMP X_m) to carry out the NMO correction. The subsequent DMO correction is, because of the assumption of a constant medium velocity, velocity independent. The fact that ray tracing is not needed to design the DMO operators makes NMO/DMO particularly attractive. As long as the medium inhomogeneities are small, NMO/DMO remains a good approximation to a 2-D MZO. Its costs fall somewhere between CMP and MZO.

It is worthwhile to stress once more the fundamental difference between the 2-D MZO and NMO/DMO stacks on the one side and the CMP and CRE stacks on the other. Whereas both former methods need some velocity assumptions to start with and yield no further information about the macrovelocity model, the CMP and CRE methods start with little or no knowledge about the medium and provide a means to construct a 2-D macrovelocity model afterward.

APPLICATION

We now present an application of the CRE method to a set of synthetic constant-offset seismic sections. These were

Table 2. Comparison of methods to construct a stacked section from a set of constant-offset sections.

Value	NMO	NMO + DMO	CRE	Direct MZO
Parameter(s) needed	—	$\bar{V}(x_m, \tau_o)$	v_o	$v(x, z)$
Needs coherency analysis	For one parameters	No	For two parameters	No
Needs ray tracing	No	No	No	Yes
Standard output	Stacked section	Prestack ZO sections	Stacked section	Prestack ZO sections
Parameter(s) estimated	$V_s(x_m, \tau_o)$	—	$R_{\text{NIP}}(x_o, \tau_o), \beta_o(x_o, \tau_o)$	—
Pulse stretch	Yes	Yes	No	Yes
Reflection-point dispersal	Full	Little	Residual	No
Amplitude preservation	No	Approximately	No	Yes
Event selection	Yes	No	No	No
Conflicting dips resolved	No	Approximately	Approximately	Yes
S/N enhancement	Good	Good	Good	Good
Macrovelocity determination	$V(z)$	No	$V(x, z)$	No

generated by ray theory for the model in Figure 8. We have simulated multicoverage reflection data from both interfaces for half-offsets $h = 0$ to $h = 0.250$ km in steps of $\Delta h = 0.01$ km and at midpoint intervals $\Delta x_m = 0.01$ km in the range $0\,\text{km} < x_m < 2.5\,\text{km}$. We have used a Gabor wavelet (Gabor, 1946) as the source signal, with its peak frequency at 80 Hz. Random noise was added to all 26 synthetic constant-offset sections to produce an S/N ratio that is similar to that in the zero-offset section shown in Figure 9.

As results of applying the CRE method, we have (1) the simulated zero-offset section, i.e., the so-called CRE stack section (Figure 10a); (2) the section with the coherency measure, i.e., the semblancegram (Figure 11a); (3) the section with the emergence angle, i.e., the anglegram (Figure 12a); and (4) the section with the radius of curvature, i.e., the radiusgram (Figure 13a). The good quality of the CRE stack section of Figure 10a is emphasized. Even in the random noise environment, the CRE stack images very well the reflection events caused by the steep flanks of the dome. For comparison, Figure 10b and 11b show the CMP stacked section obtained from the same constant-offset sections and the corresponding semblance section. The coherency sections of Figure 11 represent a kind of confidence measure for the corresponding stacked sections of

Figure 10. The higher the semblance value, the better the detected coherency of the corresponding reflection event and thus the more reliable the corresponding simulated zero-offset reflection.

The NIP-wave attributes of Figures 12a and 13a, obtained in connection with the CRE stack, are comparable to the theoretical values seen in Figures 12b and 13b, respectively. All results enable us to claim that the CRE stack is not only a useful process to simulate ZO sections without knowing the macrovelocity model, but it also allows us to determine the NIP-wave attributes (R_{NIP}, β_o) that can be used in strategies

(a) CRE stacked section

ZO section

FIG. 9. Synthetic ZO section with added random noise obtained from the seismic model in Figure 8.

FIG. 8. The seismic model is represented by a dome structure below two homogeneous layers, with velocities $v_o = 2.5$ km/s and $v_1 = 3.0$ km/s.
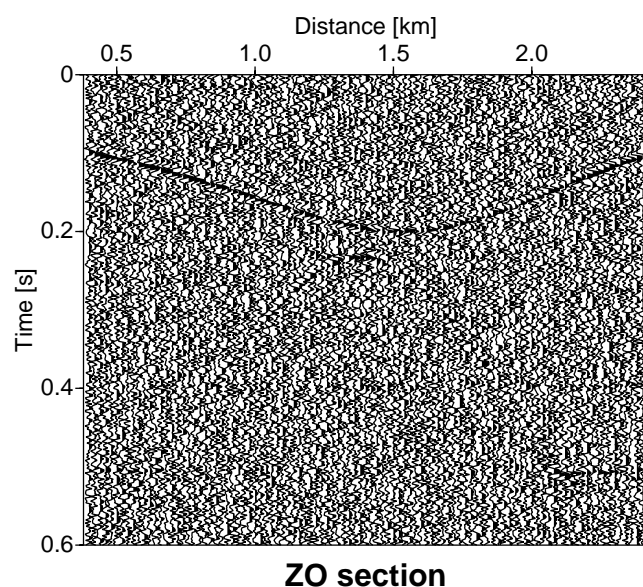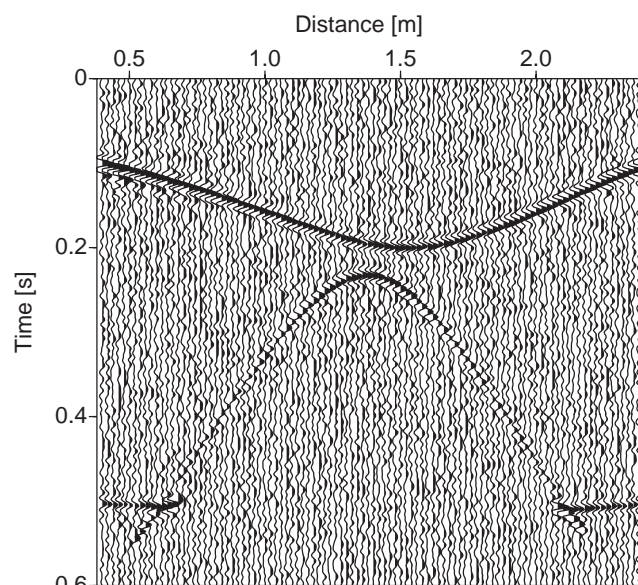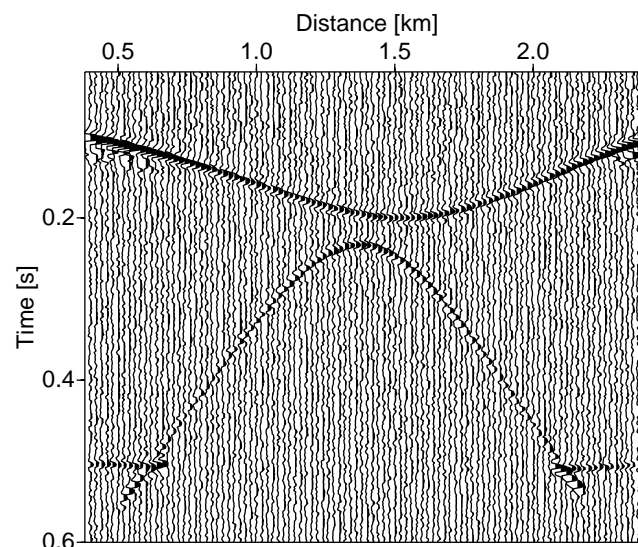

(b) CMP stacked section

FIG. 10. (a) CRE stack section obtained from the set of constant-offset sections, with S/N ratios equal to the ZO section shown in Figure 9. (b) The CMP stack section obtained from the same constant-offset sections as used for the CRE stack.

to determine the macrovelocity model (Hubral and Krey, 1980).

From the results presented above we can see the CRE stack allows us to simulate a ZO section even for a heterogeneous medium and for a rather low S/N ratio. Moreover, as a byproduct of the CRE stack, one obtains the NIP-wave parameters (radius of curvature and emergence angle) that are useful in inversion procedures to determine the macrovelocity model. In contrast, the CMP stack, with or without DMO procedure included, does not allow the construction of a laterally inhomogeneous macrovelocity model. The only result of the CMP stack is a simulated zero-offset section and a stacking-velocity-versus-depth function at every CMP.

CONCLUSIONS

In this paper, we have shown that the principal features of the CRE method consist of (a) the construction of a stacked zero-offset section from a set of constant-offset sections with only an estimate of the near-surface velocity and (b) the deter-

mination of two wavefront attributes (the radius of curvature R_{NIP} and the emergence angle β_o) for each ZO reflection in the stacked section. Both wavefront attributes can be used for traveltime inversion techniques (e.g., based on generalized Dix-type formulas) to estimate an accurate macrovelocity model.

We have also suggested an alternative scheme to construct an optimal CRE gather and its corresponding radiusgram (section of R_{NIP} values) and anglegram (section of β_o values). The somewhat complicated expressions found in the original formulation of the CRE method considering source–receiver coordinates (Gelchinsky, 1988) have been replaced by simpler expressions in terms of midpoint and half-offset coordinates. We have also shown that the CRE method is closely related to the optical stack of de Bazelaire (1988).

In summary, the CRE method has the following advantages over standard CMP stacking.

1) The seismic pulses of the ZO reflections constructed by the CRE method are not stretched when compared to true ZO reflections (i.e., the frequency of a pulse is not altered by constructing a ZO reflection in the final stacked section from a given constant-offset reflection).
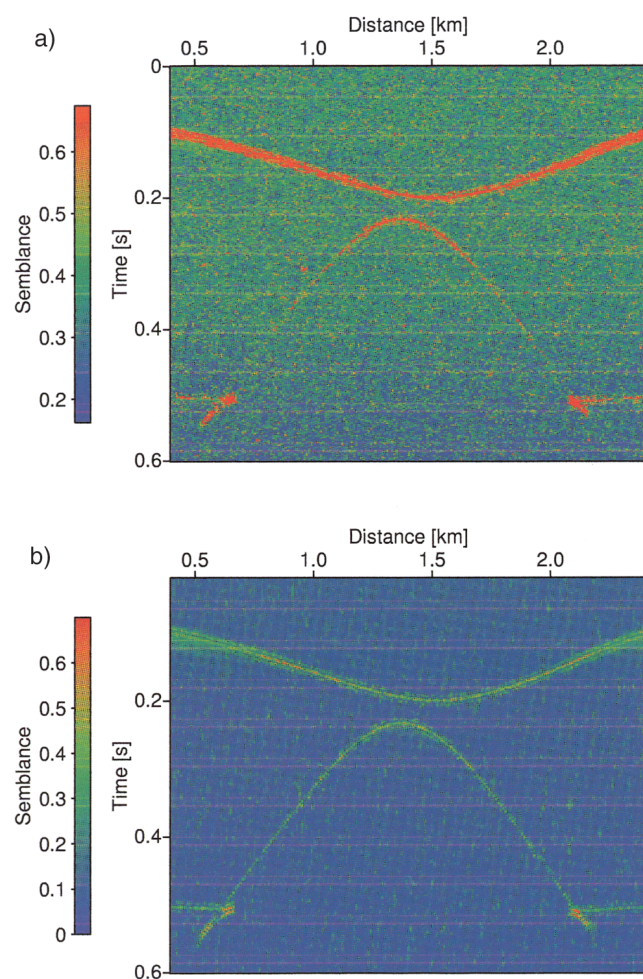

FIG. 11. (a) Semblancegram obtained for each selected time in the ZO section after applying the CRE moveout. Note the high values in the strips where the primary reflections are located. (b) The semblancegram with the semblance values obtained at each time in the ZO section after applying the NMO moveout.
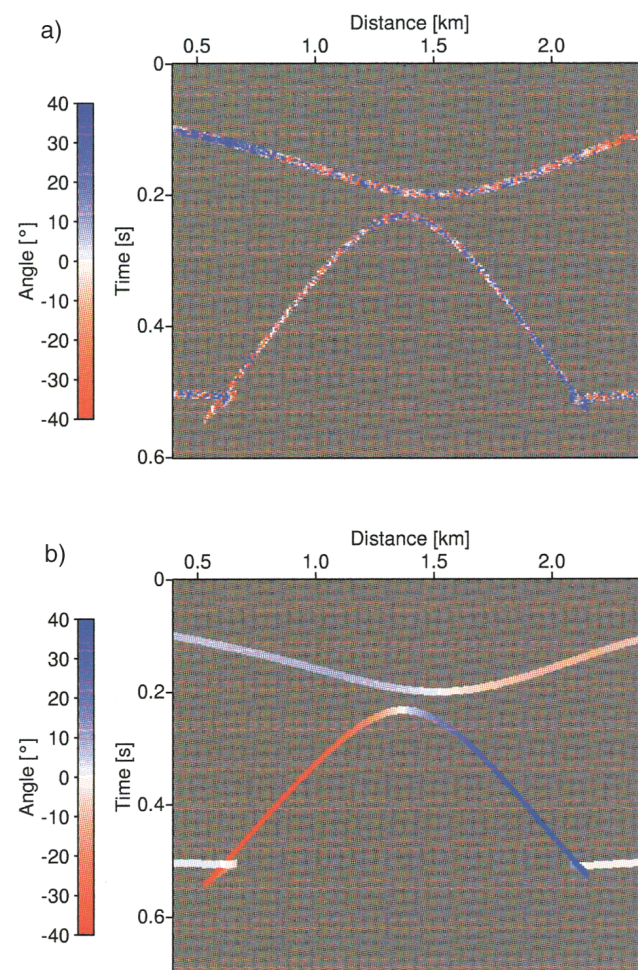

FIG. 12. Emergence angles of normal rays perpendicular to the reflectors of Figure 8: (a) obtained as a byproduct of the CRE stack; (b) obtained by forward ray tracing.

2) The CRE method, in contrast to a CMP stack, suffers from a small residual reflection-point dispersal only. Like the CMP stack, the CRE stack selects only specular primary reflections along optimally specified stacking lines.

3) A CRE gather can be constructed from a set of constant-offset sections in a parallel way as this is done from a set of common shot records. All that is needed is to transform the source–receiver coordinates into midpoint–half-offset coordinates.

4) The CRE method provides a cleaner stacked section with a better S/N ratio and a higher confidence measure (coherency).

5) Additionally to a high-quality stacked section, two (instead of one) medium parameters are obtained that can be used to estimate the velocity model better.

The main disadvantage of the CRE method in comparison to the conventional NMO/DMO method is that for each point in the stacked section a two-parameter search must be performed. Application of the CRE method to more realistic sit-

uations must show whether the benefits justify the higher costs involved. Ongoing research also includes investigations on the question of how to optimize the search.

The following implementational remarks try to answer some questions that naturally arise when applying the CRE method. In principle, one should always be suspicious of the actual implementation of the two-parameter estimation involved—in particular, with regard to the stability of the process. However, the meaningful synthetic and real data examples described in the literature attest that this is a robust process. The parameter selection has been carried out successfully in all applications, i.e., without any sophisticated coherency analysis being developed. We also remark that the two-parameter CRE moveout expression is expected, in most situations, to resolve or minimize the so-called conflicting-dip problems. In fact, the emergence angles and wavefront curvature radii are fundamental physical and geometrical attributes that are certainly better suited to separate distinct reflection events than, for example, stacking velocities obtained by a conventional CMP stack. Finally, we agree that it would be very desirable to quantify the reduction of the reflection-point dispersal achieved by the CRE method in terms of the medium inhomogeneity (e.g., values of velocity gradients). Although this is still an open question, it is rather clear that the wavefront-based treatment of the reflections provides a better dispersal reduction than the standard CMP stack.

Finally, let us remark that the CRE method is only one of various zero-offset simulation (or stacking) methods that are independent of a macrovelocity model. All of them are based on very similar geometrical considerations to the ones presented in this paper, which therefore might be regarded as an introduction to macromodel independent stacking methods. Other methods have been discussed in detail at the EAGE/SEG workshop, "Macro-model independent reflection imaging," at Karlsruhe University (February 1999). The proceedings of this workshop with approximately 10 papers constitute a special issue of the *Journal of Applied Geophysics*.
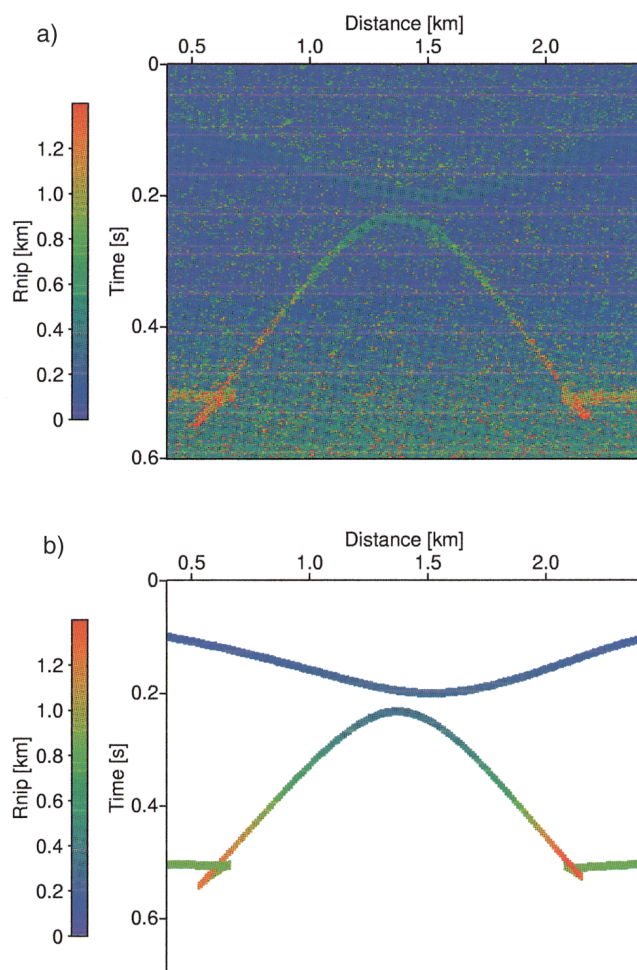

FIG. 13. Radii of curvature of the NIP waves associated with the normal rays for the reflectors of Figure 8 (a) obtained as a byproduct of the CRE stack; (b) obtained by forward ray tracing.

REFERENCES

Al-Chalabi, M., 1974, Series approximation in velocity and traveltime computations: Geophys. Prosp., **21**, 783–795.

Barnes, A. E., 1992, Another look at NMO stretch: Geophysics, **57**, 749–751.

Berkovitch, A., and Gelchinsky, B., 1989, Inversion of common reflecting element (CRE) data (migration combined with interval velocity determination): 59th Ann. Internat. Mtg., Soc. Expl. Geophys., Expanded Abstracts, 1250–1253.

Berkovitch, A., Gelchinsky, B., Keydar, S., and Shtivelman, V., 1991, Inversion of combined data of the CRE and CEE imaging (stacks): 53rd Mtg., Eur. Assn. Geosc. Eng., Abstracts, 46–47.

Berkovitch, A., Keydar, S., Landa, E., and Trachtman, P., 1998, Multifocusing in practice: 68th Ann. Internat. Mtg., Soc. Expl. Geophys., Expanded Abstracts, 1748–1751.

Bleistein, N., 1987, On the imaging of reflectors in the earth: Geophysics, **52**, 931–942.

Červený, V., 1987, Ray methods for three-dimensional seismic modelling. Lecture notes: The Norwegian Institute of Technology, University of Trondheim.

Červený, V., and Ravindra, R., 1971, Theory of seismic head waves: Univ. Toronto Press.

Cruz, J. C. R., 1994, Homeomorphic imaging of seismic reflectors: Ph.D. dissertation, Univ. Pará (in Portuguese).

———— 1997, Interval velocities inversion from seismic reflection traveltime in a 2-D earth: 5th Internat. Congress Bras. Soc. Geophys., Extended Abstracts, **2**, 625–628.

Cruz, J. C. R., and Martins, H. L., 1998, Interval velocities inversion using NIP wave attributes: 60th Ann. Internat. Mtg., Eur. Assn. Geosc. Eng., Abstracts, 1.21.

Cruz, J. C. R., Hubral, P., and Tygel, M., 1995, The CRE method: An alternative to CMP stacking: 4th Internat. Cong., Bras. Soc. Geophys., Extended Abstracts, **1**, 327–330.

Cruz, J. C. R., Hubral, P., Tygel, M., and Schleicher, J., 1996, The common-reflecting-element (CRE) method revisited: Research Report **70**, IMECC/Unicamp/Brazil.

de Bazelaire, E., 1988, Normal moveout revisited: Inhomogeneous media and curved interface: Geophysics, **53**, 143–157.

Dietrich, M., and Cohen, J. K., 1993, Migration to zero offset (DMO) for constant velocity gradient: An analytical formulation: Geophys. Prosp., **41**, 621–643.

Dix, C. H., 1955, Seismic velocities from surface measurements: Geophysics, **20**, 68–86.

French, W. S., Perkins, W. T., and Zoll, R. M., 1985, Partial migration of TRUE-3D seismic reflection surveys via common reflection point stacking: Offshore Technology Conference, **IV**, 41–67.

Gabor, D., 1946, Theory of communication: J. IEEE, **93**, 429–441.

Gelchinsky, B., 1988, The common-reflecting-element (CRE) method (non-uniform asymmetric multifold system): Expl. Geophys. **19**, 71–75.

Gelchinsky, B., Keydar, S., and Helle, H., 1993a, Studying of salt dome by homeomorphic imaging technique: A case history: 55th Ann. Internat. Mtg., Eur. Assn. Geosc. Eng., Abstracts, P110.

———— 1993b, Structural imaging of a salt dome by using homeomorphic methods: Seismo-series **59**, Inst. Solid Earth Physics, Univ. Bergen.

Gelchinsky, B., Landa, E., and Shtivelman, V., 1985, Algorithms of phase and group correlation: Geophysics, **50**, 595–608.

Goldin, S. V., 1986, Seismic traveltime inversion: Investigations in geophysics **1**, Soc. Expl. Geophys.

Hale, D., 1991, Dip moveout processing, *in* Domenico, S. N., Ed., Course notes series, **4**: Soc. Expl. Geophys.

Höcht, G., de Bazelaire, E., Majer, P., and Hubral, P., 1999, Seismics and optics: Hyperbolae and curvatures. J. Appl. Geoph., **42**, 261–281.

Hubral, P., 1983, Computing true-amplitude reflections in a laterally inhomogeneous earth: Geophysics, **48**, 1052–1063.

Hubral, P., and Krey, T., 1980, Interval velocities from seismic reflection time measurements: Soc. Expl. Geophys.

Keydar, S. 1994, New method of homeomorphic stacking and imaging of seismic data: Ph.D. dissertation, Tel-Aviv Univ.

Keydar, S., Edry, D., Berkovitch, A., and Gelchinsky, B., 1995, Construction of a kinematic seismic model by the homeomorphic imaging method: 57th Ann. Mtg., Eur. Assn., Expl. Geophy., Extended Abstracts, P086.

Koren, Z., and Gelchinsky, B., 1989, Common-reflecting-element (CRE) ray tracing for the calculation of the global multi-offset time field: Geophys. J. Internat., **99**, 391–400.

Kravtsov, Y. A., and Orlov, Y. I., 1990, Geometrical optics of inhomogeneous media: Springer-Verlag Publ. Co., Inc.

Levin, F. K., 1971, Apparent velocity from dipping interface reflections: Geophysics, **36**, 510–516.

Liptow, F., and Hubral, P., 1995, Migrating around in circles: Leading Edge, **14**, 1125–1127.

Müller, T., Jäger, R., and Höcht, G., 1998, Common reflection surface stacking method—Imaging with an unknown velocity model: 68th Ann. Internat. Mtg., Soc. Expl. Geophys., Expanded Abstracts, 1764–1767.

Neidell, N. S., and Taner, T., 1971, Semblance and other coherency measures for multichannel data: Geophysics, **36**, 482–497.

Olalde, C. C. B., 1996, The common-reflecting-element (CRE) method applied to the analysis of complex seismic reflectors: Ph.D. dissertation, Kiel Univ.

Perroud, H., Hubral, P., Höcht, G., and de Bazelaire, E., 1996, Common-reflection-point stacking in laterally inhomogeneous media: 66th Ann. Internat. Mtg., Soc. Expl. Geophys., Expanded Abstracts, 495–498.

Rabbel, W., Bittner, R., Gelchinsky, B., 1991, Seismic mapping of complex reflectors with the common-reflecting-element method (CRE method): Phys. Earth Plan. Internat., **67**, 200–210.

Schleicher, J., Hubral, P., Höcht, G., and Liptow, F., 1997, Seismic constant-velocity remigration: Geophysics, **62**, 589–597.

Schleicher, J., Tygel, M., and Hubral, P., 1993, 3-D true-amplitude finite-offset migration: Geophysics, **58**, 1112–1126.

Schneider, W. A., 1978, Integral formulation for migration in two and three dimensions: Geophysics, **43**, 1043–1073.

Steentoft, H., 1993, Imaging of reflection seismic data with the common-reflecting-element method: Ph.D. thesis, Kiel Univ.

Steentoft, H., Goedde, W., and Thiel, M., 1992, The power of reflection seismics for mapping of shallow layers: 54th Ann. Internat. Mtg., Eur. Assn. Expl. Geophys., Extended Abstracts, 730–731.

Steentoft, H., and Rabbel, W., 1992a, Processing of complex data with the CRE method: 54th Ann. Internat. Mtg., Eur. Assn. Geosc. Eng., Abstracts, 560–561.

———— 1992b, The CRE method: A technique of homeomorphic imaging in processing of seismic data: Acous. Imag., **19**, 803–809.

———— 1994, Seismic mapping of the Marmousi data set with the common reflecting element method (CRE method): Tectonophysics, **232**, 355–363.

Stolt, R. H., 1978, Migration by Fourier transform: Geophysics, **43**, 23–48.

Taner, M. T., and Koehler, F., 1969, Velocity spectra—Digital computer derivation and application of velocity function: Geophysics, **34**, 859–881.

Tygel, M., Schleicher, J., Hubral, P., and Santos, L. T., 1998, 2.5-D true-amplitude Kirchhoff migration to zero-offset in laterally inhomogeneous media: Geophysics, **63**, 557–573.

Vermeer, G. J. O., 1990, Seismic wavefield sampling: Soc. Expl. Geophys.

Yilmaz, O., 1987, Seismic data processing: Soc. Expl. Geophys.

APPENDIX

GELCHINSKY'S FORMULAS

All previous papers on the CRE method (e.g., Koren and Gelchinsky, 1989; Rabbel et al., 1991) start from the assumption that sources and receivers are asymmetrically distributed in a CRE gather, approximately obeying the binomial distribution rule (in our notation)

$$x_s = x_o - Y(1 + \alpha Y), \qquad (A\text{-}1)$$

$$x_g = x_o + Y(1 - \alpha Y). \qquad (A\text{-}2)$$

This approximation is only valid for small values of α. By eliminating Y from equations (A-1) and (A-2), one obtains the following formula for the asymmetry factor:

$$\alpha = 2\frac{2x_o - x_s - x_g}{(x_g - x_s)^2}. \qquad (A\text{-}3)$$

Koren and Gelchinsky (1989) show that, for a given source position x_s, parameter Y can be computed from

$$Y = \frac{\sqrt{1 + 4\alpha(x_o - x_s)} - 1}{2\alpha}, \qquad (A\text{-}4)$$

which is obtained by solving equation (A-1) for Y. Substituting this expression into equation (A-2) yields the receiver position x_g, which corresponds to the given source position x_s. Note, however, that computing Y from equation (A-4) may be very unstable for small parameters α.

The CRE moveout (also called the oblique spherical correction by Gelchinsky and co-workers) relative to the source–receiver pair (S, G) in the CRE gather as determined in this way can then be expressed in terms of the quantity Y as

$$\Delta\hat{\tau} = \frac{2R_{\text{NIP}}}{v_o}\left\{\sqrt{1 - Y^2\left(\alpha^2 - 1/R_{\text{NIP}}^2\right)} - 1\right\}. \qquad (A\text{-}5)$$

This approximate equation for the moveout $\Delta\hat{\tau}$ differs from our equations (8) and (16), which are exact for a constant-velocity medium as long as equations (10) and (14), respectively, are used to determine x_g from x_s or x_m from h. Equation (A-5) is mathematically equivalent to equation (16) if the approximate rule (15) is used to compute x_m from h. However, even in this approximation equation (A-5) may be computationally more problematic because of the use of the parameter Y.

From the above, we may draw the following conclusions. Working with the alternative CRE stacking formula (16), instead of the original one, equation (A-5) introduced by Gelchinsky and co-workers (see Koren and Gelchinsky, 1989; Rabbel et al., 1991) has advantages. First, the parameter Y is not required to determine the auxiliary CRE gather. This is important because Y, given by equation (A-4), has as its denominator the asymmetry factor α for which usually $|\alpha| \ll 1$. This in turn means that small deviations of the numerator of Y are amplified, so that Y is an unstable parameter. Because our strategy does not require the parameter Y, this should make the CRE method more attractive as an imaging tool and also with respect to computing more stable radiusgrams and anglegrams. As a consequence, one should also obtain more stable macrovelocity models. Second, auxiliary CRE gathers are more quickly constructed from a set of constant-offset sections rather than neighboring shot records. For each point X_o on the seismic line and for each fixed α, the midpoint coordinate x_m in a constant-offset section with half-offset h is immediately determined by formula (15). Thus, the pair (x_m, h) of any seismic trace in the CRE gather is defined completely.